

Surface proofs for linear logic

Lawrence Dunn
North Florida Community College
dunnl@nfcc.edu

Jamie Vicary
University of Oxford
jamie.vicary@cs.ox.ac.uk

January 20, 2016

We show that a proof in multiplicative linear logic can be represented as a decorated surface, such that two proofs are logically equivalent just when their surfaces are geometrically equivalent. The technical basis is a coherence theorem for Frobenius pseudomonoids.

1 Introduction

Multiplicative linear logic [9, 7] is a formal calculus for reasoning about resources, which is similar to traditional logic, except that resources cannot be duplicated or neglected in the way that propositions can.

A central problem in logic is determining when two proofs should be considered equivalent. In this paper, we describe a scheme for interpreting proofs in multiplicative linear logic as *geometrical surfaces* embedded in 3d space. We define two surfaces as *equivalent* just when one can be deformed into the other, in sense we make precise. Our main theorem then reads as follows.

Theorem 2.2. *Two sequent proofs in multiplicative linear logic have equal interpretations in the free $*$ -autonomous category just when their surfaces are equivalent.*

The theory of $*$ -autonomous categories [25, 22] is a standard mathematical model for linear logic, so this theorem says that the notion of proof equality provided by the surface calculus agrees with the standard one.

Our surfaces are similar in spirit to *proof nets* [9, 5], graphical structures which are used in linear logic to denote proofs. However, we argue that our scheme has several advantages:

1. Correctness is local; any well-typed composite produces a valid proof-theoretic object, with no global property (such as the *long-trip criterion* [9]) to be verified.
2. Equivalence is local, unlike for proof nets where the main dynamical rewiring step involves non-local jumps, and requires the re-validation of a global property [5, Section 3.1].
3. Equivalence is broad, establishing some proof equivalences in fewer steps than for proof nets; sometimes in just one step.

4. It works well with the unital fragment of the logic, which is problematic for traditional proof nets, requiring decorations in the form of *thinning links* [5].
5. It is compositional, in the sense that the surface for a composite proof is just the union of the surfaces for any partition.
6. It is close to categorical semantics, with a surface giving rise straightforwardly to a morphism in a $*$ -autonomous category.

To our knowledge, no approach to proof nets has all these desirable properties (although see the discussion in Section 1.1.)

However, despite these differences, the formalisms are intimately connected, in the following way: the proof net is the 2d *projection* of the 3d surface geometry. From this perspective, we can make sense of some of the features of proof nets: the long-trip criterion can be interpreted as a non-local check that the 2d shadow is consistent with a valid 3d geometry, and the thinning link decorations indicate the depth at which a unit is attached in the 3d geometry.

The core technical contribution is a coherence theorem for Frobenius pseudomonoids, which shows that all diagrams of a certain sort commute. This immediately implies a new coherence theorem for $*$ -autonomous categories.

We criticise our scheme in the following ways. When we say in point 4 above that it works well with the unital fragment of the logic, we mean that the notion of proof equivalence is straightforward and local, not that one obtains an efficient method for deciding proof equality; this is known to be impossible [11]. We work in a non-symmetric variant of the logic which lacks the exchange rule; adding a symmetry would mean that the surfaces self-intersect, which would complicate the formalism, although we expect our results could be extended. Also, as complex geometrical objects, our surfaces are not as easy to manipulate with pen-and-paper as traditional proof nets; to be practical, advances in proof assistant technology (such as [1]) will be required.

1.1 Related work

It is well-recognized that ideas from topology are relevant for linear logic. The original proof nets of Girard [9] are topological objects, and Melliès has shown how the topology of ribbons gives a decision procedure for correctness of proof nets [21]. Proof nets allow reasoning about proofs with units, but the formalism is complex, requiring a system of thinning links with moving connections [5]. Hughes [14] gives a variant of proof nets which works well with units, satisfying properties 4 and 5 above, but lacking properties 1, 2, 3, and 6. Our approach has a local flavour which is shared by the deep-inference model of proof analysis [10] and the access to monoidal coherence that it allows [13]; however, our coherence theorem is strictly more powerful, as it operates in a fragment that combines the \otimes and \wp connectives. We note also the work of Slavnov [26] on linear logic and surfaces, which involves some similar ideas to the present article, but is technically quite different.

1.2 Outline

We begin in Section 2 by describing the surface calculus, and giving a systematic method for translating traditional sequent calculus proofs into this scheme. We

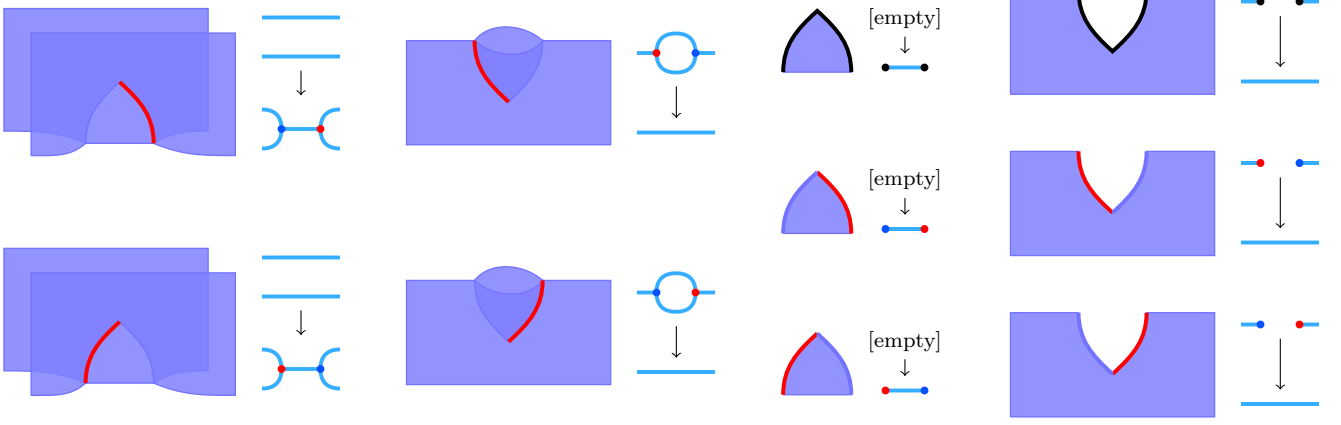


Figure 1: The generators of the 3d calculus

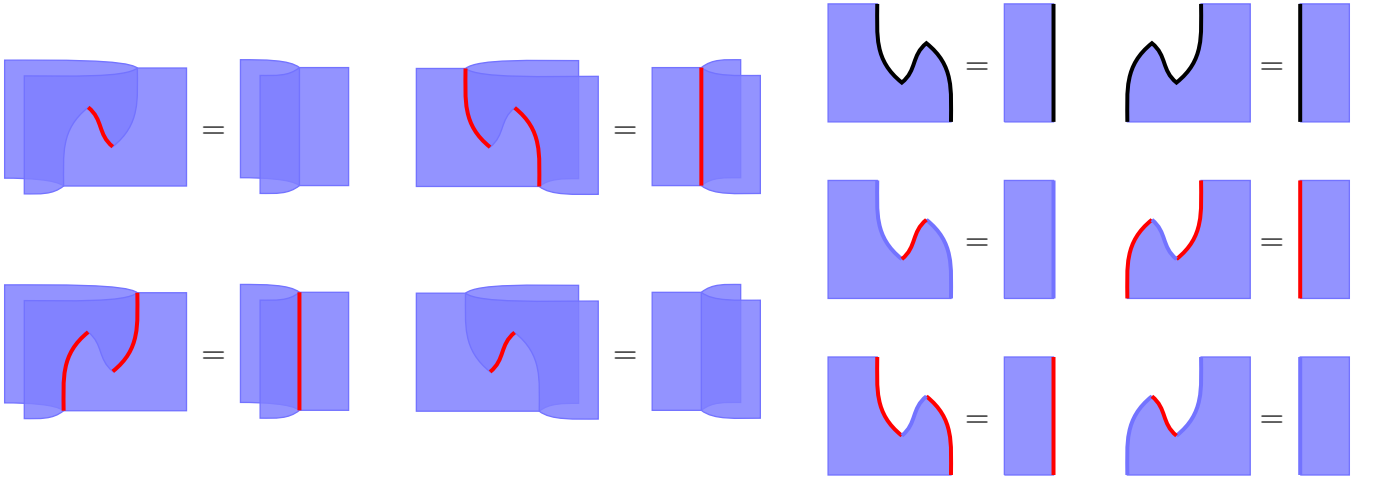


Figure 2: The equations of the 3d calculus

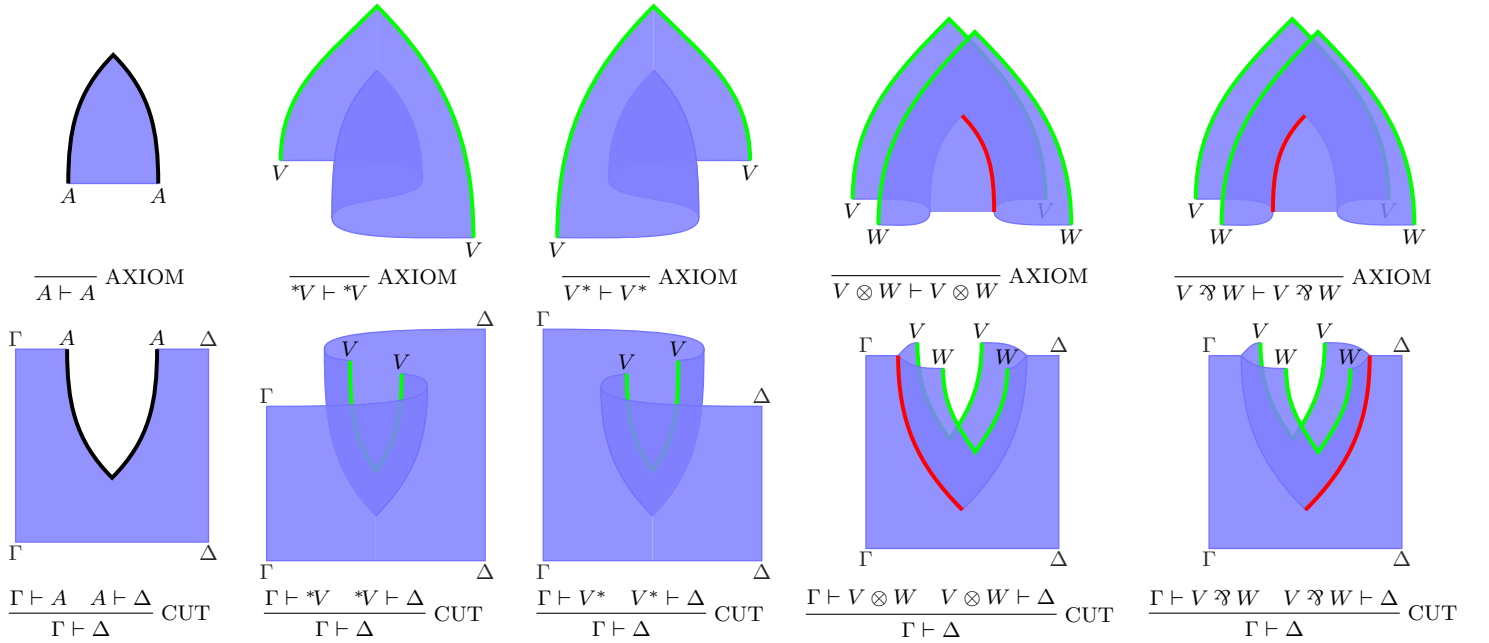


Figure 3: AXIOM and CUT rules for an atomic variable A , and recursively for variables V, W

also formally state our main result, and show how proof nets are a projection of the surface calculus. In Section 3 we illustrate our formalism through a range of examples: we derive the form of an additional logical rule; we deduce a proof equality involving units, comparing it to the proof net analysis; and we analyze the classic triple-dual problem. In Section 4 we prove our main technical result on coherence for Frobenius pseudomonoids, and deduce our main theorem as a corollary. The central higher-categorical arguments are verified with the web-based proof assistant *Globular* [1], with direct links provided to the formalized proofs. An Appendix gives some additional proofs.

This article is designed to be viewed in colour, as much of the typing information in the diagrams will be invisible in grayscale.

1.3 Acknowledgements

The authors are grateful to Samson Abramsky, Nick Gurski and Sam Staton for useful comments. 3d graphics have been written in *TikZ*, and 2d graphics have been produced by the proof assistant *Globular* [1].

2 Surface calculus

In this section we develop the 2d string diagram calculus for sequents, and the 3d surface calculus for proofs. We show how to translate a sequent calculus proof into the surface calculus, and we define the equivalence relation on surfaces.

2.1 The 2d calculus

The 2d calculus, which we will use to represent individual sequents, is the Joyal-Street calculus for monoidal categories [17], directed from left to right. We use the standard 2-sided sequent calculus for nonsymmetric multiplicative linear logic with units [5]: our sequents are pairs $\Gamma \vdash \Delta$, where Γ and Δ are ordered lists (separated with “,”) of expressions in the following grammar, where $V = \{A, B, C, \dots\}$ is a set of atomic variables:

$$S ::= \{I, \perp\} \mid V \mid S \otimes S \mid S \wp S \mid S^* \mid {}^*S$$

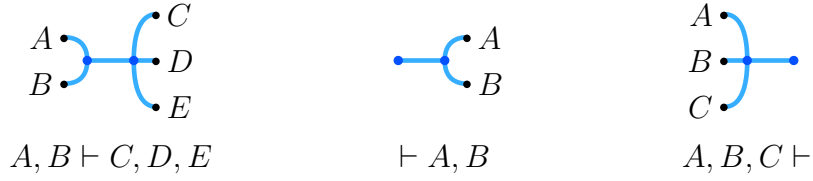
We have left and right negation, and isomorphisms ${}^*(S^*) \simeq S \simeq ({}^*S)^*$ are a native part of the calculus (see Example 3.3.)

Our graphical language for sequents is as follows. Atomic variables are represented as black dots, pointing in different directions depending on their side of the sequent:

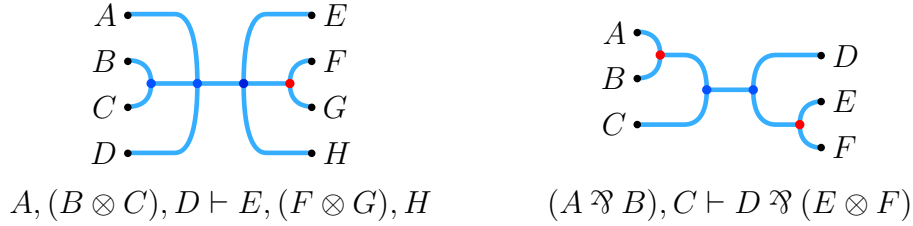
$$\begin{array}{cc} A \bullet \text{---} \dots & \dots \text{---} \bullet A \\ A \vdash \dots & \dots \vdash A \end{array}$$

The two sides of a sequent are represented graphically by trees, which are drawn connected together at their roots. The basic connective “,” is denoted as a blue

vertex with zero or more branches to the left or right, as follows:



The connectives \otimes and \wp , which are always binary, are drawn in blue on their natural side (left for \otimes , right for \wp), and in red on the other side, as we show with the following examples:

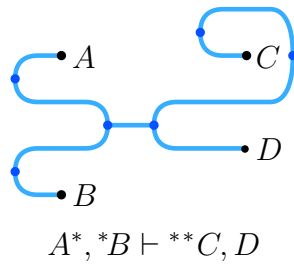


Note that a blue dot with a binary branching is therefore an overloaded notation; this is a deliberate feature.

The units I and \perp are represented by blue dots on their natural side (left for I , right for \perp), and red dots on the other side, as shown:



We represent $(-)^*$ as turning right by a half-turn, and $*(-)$ as turning left by a half-turn, as shown:

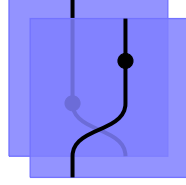


Diagrams built from sequents in this way are of a simple kind; as graphs, they are all acyclic and connected. In general we can allow arbitrary well-typed composites of these components; such diagrams represent 1-morphisms in the monoidal bicategory $\mathbf{F}(\mathcal{F}^*)$, described in Section 4.

2.2 The 3d calculus

Diagrams in the 3d calculus are surfaces embedded in \mathbb{R}^3 . Formally they are expressions in the graphical calculus for Gray categories, which is by now well-developed [3, 16, 24, 4]. However, the 3d calculus is quite intuitive, and we take advantage of this to introduce it in an informal way.

Diagrams consist of *sheets*, bounded on the left and right by *edges*, which are bounded above and below by *vertices*. (Sheets can also be bounded by the sides of the diagram, and edges can also be bounded by the top or bottom of the diagram.) Diagrams are immersed in 3d space, meaning that sheets can exist in front or behind other sheets, and wires on sheets of different depths can cross; however, components never intersect. Here is an example:



Here we have front and back sheets, each containing an edge, which contains a vertex. Towards the bottom of the picture, the wires cross: this is called an *interchanger*.

For our application to linear logic, we allow two types of vertex: *coherent vertices* and *adjunction vertices*.

- **Coherent vertices.** Say that a 2d calculus diagram is *simple* when it is connected and acyclic with nonempty boundary, and in the blue fragment of the calculus, not involving red nodes or black atomic variable nodes. Then any two simple diagrams can be connected by a coherent vertex, denoted as follows:



On the left we give the surface representation, and on the right we give the 2d calculus representation of the upper and lower boundaries. The coherent vertex is the point in the middle of the surface diagram where 4 edges meet.

- **Adjunction vertices.** Listed in Figure 1, these introduce and eliminate red and black edges in the surface calculus.

We now define equivalence in the graphical language, giving intuitive interpretations of each generating relation in *italics*.

Definition 2.1. Two surface diagrams are *equivalent* when they are related by the least equivalence relation generated by the following:

- **Coherence.** Let P, Q be surface diagrams built from interchangers and geometry vertices, whose upper and lower boundaries are simple 2d diagrams; then $P = Q$. (*All acyclic equations of coherent vertices hold.*)
- **Adjunction.** The equations listed in Figure 2 hold. (*Bent wires can be pulled straight.*)
- **Isotopy.** The equations of a monoidal bicategory hold. (*If two diagrams are ambient isotopic, they are equivalent.*)

- **Locality.** Suppose surface diagrams P, Q differ only with respect to subdiagrams P', Q' , with $P' = Q'$. Then $P = Q$. (*Equivalence applies locally in the interior of a diagram.*)

It is a fair summary of this definition to say that two diagrams are equivalent just when one can be *deformed* into the other.

Our presentation here is informal, but we emphasize that our definition of the surface calculus and its equivalence relation can be made completely precise in terms of the formal development of Section 4: two diagrams are equivalent just when they are equal as 2-morphisms in the monoidal bicategory $\mathbf{F}(\mathcal{F}^*)$.

2.3 Interpreting the sequent calculus

We saw in Section 2.1 how individual sequents in multiplicative linear logic can be interpreted as 2d diagrams. We now see how proofs can be interpreted as 3d surface diagrams. We view these surfaces as directed from top to bottom, just like traditional sequent calculus proofs; so for a particular surface, its *hypothesis* is the upper boundary, and its *conclusion* is the lower boundary.

We use a basis for the sequent calculus with a symmetry between introduction and elimination for \otimes , \wp , I and \perp ; the rules \otimes -R, \wp -L, I -R and \perp -L are derivable (see Example 3.1.) The interpretation of AXIOM and CUT rules are given recursively in Figure 3; the interpretation of the remaining rules, which we call the *core fragment* of the logic, is given in Figure 4.

We now state our main theorem.

Theorem 2.2. *Two sequent proofs in multiplicative linear logic have equal interpretations in the free $*$ -autonomous category just when their surface diagrams are equivalent.*

The proof will follow at the end of Section 4.

It is interesting to analyze the different contributions to proof equivalence made by each part of Definition 2.1 of surface equivalence. **Coherence** tells us that any two proofs built in the core part of the logic given in Figure 4 are equal. **Adjunction** tells us that AXIOM and CUT cancel each other out, both for atomic and compound variables. **Isotopy** tells us that that ‘commutative conversion’ is possible, where we exchange the order of multiple independent hypotheses. **Locality** tells us that we can apply our equations in the context of a larger proof, in the manner of deep inference [10].

We give a formal statement of coherence for the core part of the logic, since it is a result of independent interest. Note that this is not a theorem about the surface calculus, although its proof uses the surface calculus.

Corollary 2.3. *If two sequent proofs in the core fragment of the logic given in Figure 4 have the same hypotheses and conclusion, then they are equal in the free $*$ -autonomous category.*

We comment on some interesting features of the translation between the sequent calculus and the surface calculus. The fundamental simplicity of the surface calculus is clear, from the minimality of the data in Figure 1, as compared to Figures 3 and 4. Partly this is achieved by the greater degree of locality: for example, the cut rules

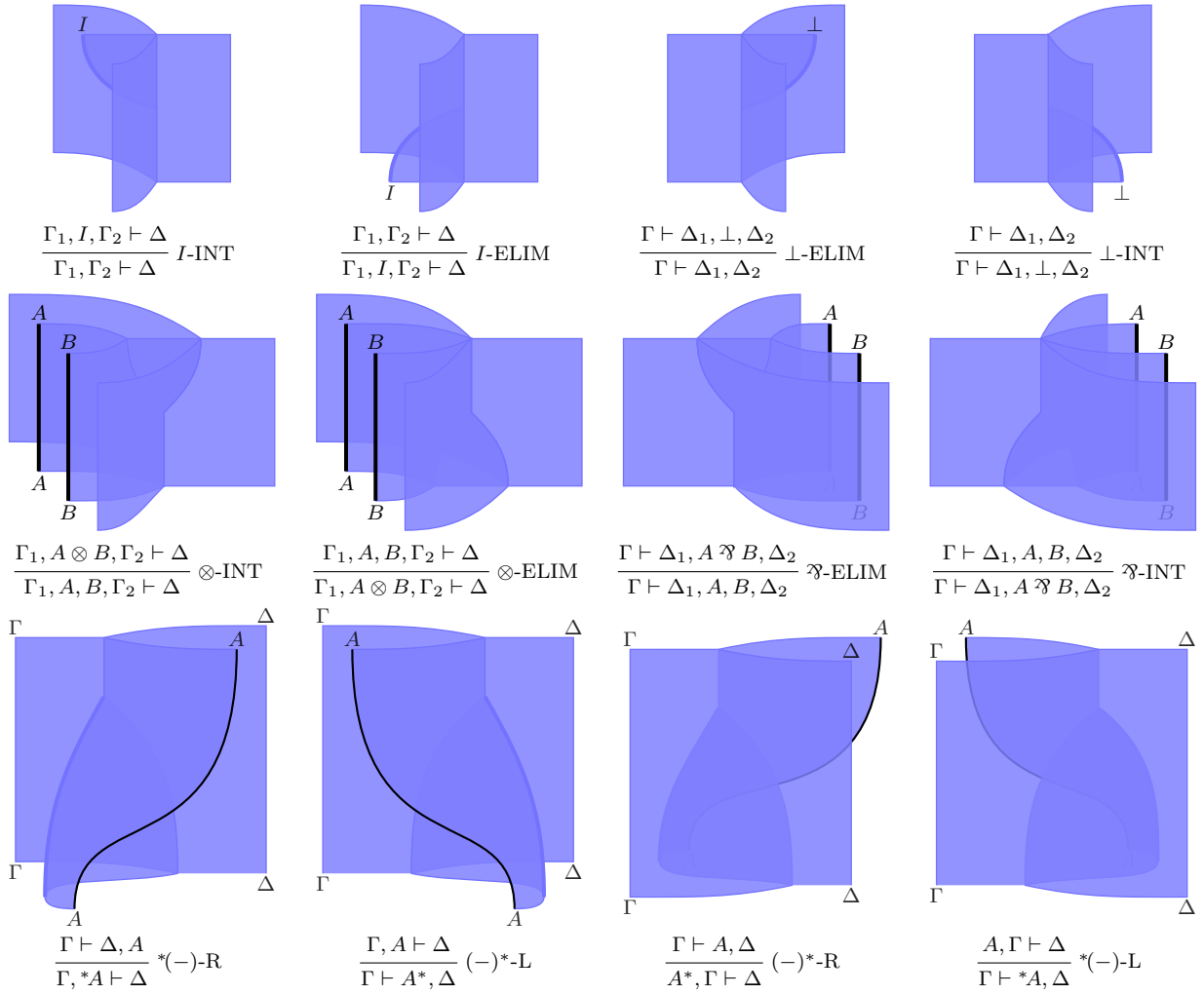


Figure 4: Surface interpretations of the core logical rules

for $*V$ and V^* are both interpreted using the same surface generators, composed in different ways. But more significantly, the entire core fragment of the sequent calculus is interpreted in the *trivial* part of the surface calculus, significantly reducing the bureaucracy of proof analysis, to use Girard's phrasing [9]. To make the most of these advantages, we suggest that the surface calculus can serve directly as a toolkit for logic, not just as a way to visualize sequent calculus proofs.

3 Examples

In this Section, we look in detail at a number of examples: we derive the surface form of the missing $\otimes\text{-R}$ rule; we analyze equivalence of a proof involving units; and we investigate the classic triple-unit problem.

Example 3.1 (Additional rules). Presentations of multiplicative linear logic usually include the rules $\otimes\text{-R}$, $\wp\text{-L}$, $I\text{-R}$, $\perp\text{-L}$, which are missing from Figure 3 and Figure 4; however, they are derivable. We analyze $\otimes\text{-R}$ in detail in Figure 6. On the left-hand side, we derive the rule in our chosen basis for the sequent calculus. In the middle image, we interpret it in the surface calculus, using the rules we have described. In

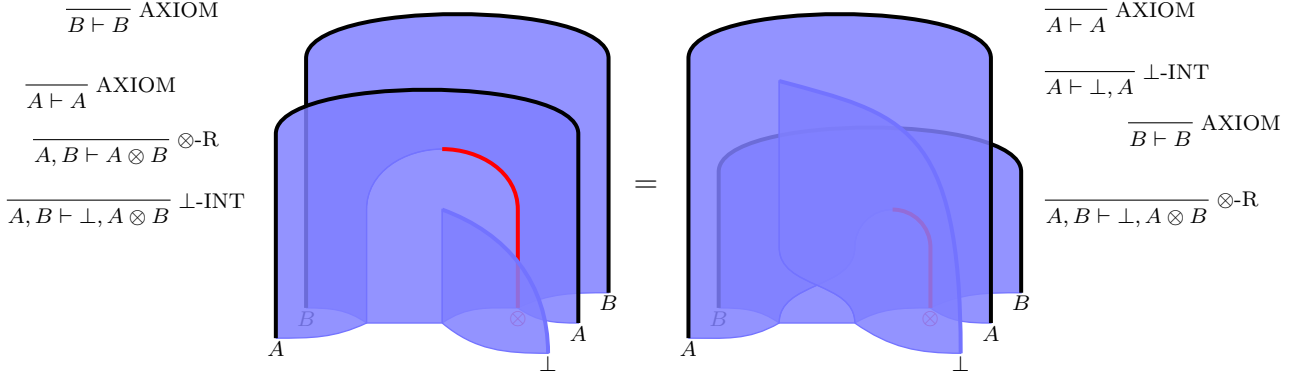


Figure 5: Geometrical equivalence of two proofs in involving the unit

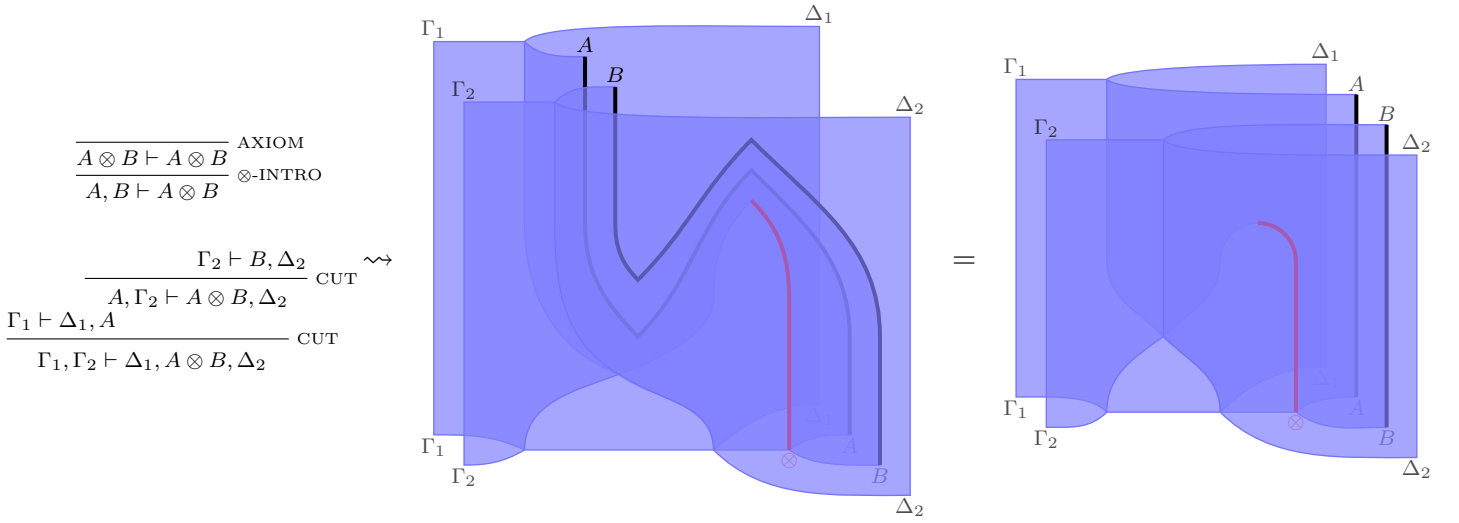


Figure 6: Derivation of the surface representation of the \otimes -R rule

the third image, we simplify the surface calculus interpretation using the rules in Figure 2. From this simplified diagram, we see that it does not in fact involve the variables, the nontrivial generators being applied in the central part of diagram only. Elegant interpretations of the other 3 rules can be derived similarly.

Example 3.2 (Equivalence of two proofs with units). The example is given in Figure 6. We present two distinct sequent proofs of the tautology $A, B \vdash \perp \wp(A \otimes B)$, along with their corresponding surface proofs. The heights are aligned to help understand how the surface proofs have been constructed. We make use of the \otimes -R rule derived in the previous example.

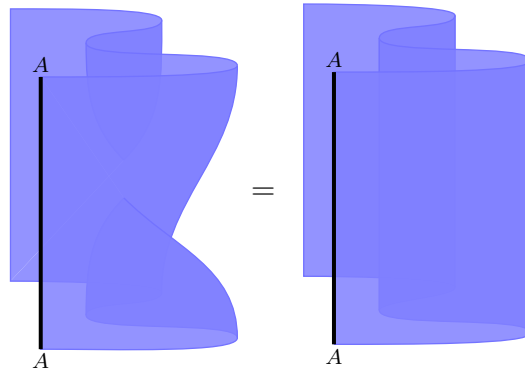
It can be seen by inspection that the surface proofs are equivalent, as follows. Starting with the surface on the left, we allow the \perp -introduction vertex to move up and to the left; this is an application of **Coherence** and **Locality**. We also allow the B -introduction vertex at the top of the diagram to move down, behind both the A -introduction and \perp -introduction vertices; this is an application of **Isotopy**.

Example 3.3 (Triple-unit problem). Starting with the identity $A \multimap X \rightarrow A \multimap X$, we can uncurry on the left to obtain a morphism $A \otimes (A \multimap X) \rightarrow A$, and curry on the right to obtain a morphism $p_A : A \rightarrow X \multimap (A \multimap X)$; in a similar way, we can

also define a morphism $q_A : A \rightarrow (X \multimap A) \multimap X$. Then the *triple-unit problem*, originally due to Kelly and Mac Lane [18] and generalized here to the non-symmetric setting, is to determine whether the following equation holds:

$$\begin{array}{ccc}
 X \multimap ((X \multimap A) \multimap X) & \xrightarrow{X \multimap q_A} & X \multimap A \\
 & \searrow \text{id} & \downarrow p_{X \multimap A} \\
 & & X \multimap ((X \multimap A) \multimap X)
 \end{array} \tag{2}$$

Choosing $X = \perp$, then q_A and p_A are the isomorphisms $*(A^*) \simeq A \simeq (*A)^*$. We give the surfaces for the clockwise and anticlockwise paths of (2):



$$\tag{3}$$

We conclude that the proofs are equivalent by a *single* application of the **Coherence** rule. Contrast this with the treatment of Blute et al [5, Section 4.2] and Hughes [15, Example 2] in terms of proof nets, where the proofs require several rewiring steps.

4 Coherence for Frobenius pseudomonoids

In this section we prove the coherence theorem for Frobenius pseudoalgebras, our main technical result. The mathematical setting is higher algebraic structures in finitely-presented monoidal bicategories. This section is more technical than the earlier part of the paper, but we give intuitive accounts of the development where possible.

For reasons of space, our string diagrams in this section run bottom-to-top. Also, it is convenient to only allow *generic composites* of 1- and 2-morphisms, meaning that composite 1- and 2-morphisms have a definite length, and a linear order on their components, from ‘first’ to ‘last’; this is without loss of generality (see [4] and [8, Section 2.2].) As a point of notation, we write $\xrightarrow{\sim}$ to denote an interchanger 2-morphism, and $\xrightarrow{\sim}$ to denote a composite of interchangers of length at least 0.

4.1 Definitions

Just as we can present a monoid by generators and relations, and a monoidal category by a PRO [20], a similar approach can be used for monoidal bicategories, as developed in the thesis of Schommer-Pries [24, Section 2.10].

- Invertible 2-morphisms μ and ν :

$$\begin{array}{ccc} \text{Diagram 1} & \xrightarrow{\mu} & \text{Diagram 2} \end{array} \quad \begin{array}{ccc} \text{Diagram 3} & \xrightarrow{\nu} & \text{Diagram 4} \end{array}$$

- Swallowtail equations:

$$\begin{array}{lcl} \text{id} & = & \text{Diagram 1} \xrightarrow{\mu^{-1}} \text{Diagram 2} \approx \text{Diagram 3} \xrightarrow{\nu} \text{Diagram 4} \\ \text{id} & = & \text{Diagram 5} \xrightarrow{\mu^{-1}} \text{Diagram 6} \approx \text{Diagram 7} \xrightarrow{\nu} \text{Diagram 8} \end{array}$$

The swallowtail equations are actually redundant, in the sense that any Frobenius pseudomonoid that violates them gives rise to one that satisfies them [23], but for simplicity we include them.

We can now state our main technical theorem.

Definition 4.5. A 1-morphism in $\mathbf{F}(\mathcal{F})$ is *connected* or *acyclic* when its string diagram graph is connected or acyclic respectively.

Theorem 4.6 (Coherence for Frobenius structures). *Let $P, Q : X \rightarrow Y$ be 2-morphisms in $\mathbf{F}(\mathcal{F})$, such that X is connected and acyclic, with nonempty boundary. Then $P = Q$.*

Thus, as long as one restricts to connected, acyclic diagrams with boundary, “all diagrams commute”. The proof strategy is to “rotate” 2-morphisms in $\mathbf{F}(\mathcal{F})$ so that they are equal to 2-morphisms in $\mathbf{F}(\mathcal{P})$, and then rely on coherence for pseudomonoids.

4.2 Rotations and twistedness

Definition 4.7. The *extended Frobenius signature* \mathcal{E} is the same as \mathcal{F} , with the following additional data:

- Morphism $\text{cap} : \mathbf{C} \boxtimes \mathbf{C} \rightarrow \mathbf{1}$:



- Invertible 2-morphism π :

$$\text{Diagram 1} \xrightarrow{\pi} \text{Diagram 2}$$

- 2-Morphisms σ_1 , σ_2 , σ_1^{-1} and σ_2^{-1} , called the *snakeorators* and *inverse snakeorators*, equipped with additional equations as follows:

$$\begin{array}{ll} \sigma_1 = \text{Diagram 1} \xrightarrow{\pi} \text{Diagram 2} \xrightarrow{\mu} \text{Diagram 3} & \sigma_1^{-1} = \text{Diagram 4} \xrightarrow{\pi^{-1}} \text{Diagram 5} \xrightarrow{\mu^{-1}} \text{Diagram 6} \\ \sigma_2 = \text{Diagram 7} \xrightarrow{\pi} \text{Diagram 8} \xrightarrow{\nu} \text{Diagram 9} & \sigma_2^{-1} = \text{Diagram 10} \xrightarrow{\pi^{-1}} \text{Diagram 11} \xrightarrow{\nu^{-1}} \text{Diagram 12} \end{array}$$

- 2-Morphisms $R_m, L_m, R_u, L_u, R_f, L_f$, with additional equations as follows:

$$\begin{aligned}
R_m &= \text{[diagram]} \xrightarrow{\sigma_1^{-1}} \text{[diagram]} \simeq \text{[diagram]} \xrightarrow{\pi} \text{[diagram]} \xrightarrow{\alpha} \text{[diagram]} \xrightarrow{\pi^{-1}} \text{[diagram]} \\
L_m &= \text{[diagram]} \xrightarrow{\sigma_2^{-1}} \text{[diagram]} \simeq \text{[diagram]} \xrightarrow{\pi} \text{[diagram]} \xrightarrow{\alpha^{-1}} \text{[diagram]} \xrightarrow{\pi^{-1}} \text{[diagram]} \\
R_u &= \text{[diagram]} \xrightarrow{\sigma_1^{-1}} \text{[diagram]} \simeq \text{[diagram]} \xrightarrow{\pi} \text{[diagram]} \xrightarrow{\lambda} \text{[diagram]} \\
L_u &= \text{[diagram]} \xrightarrow{\sigma_2^{-1}} \text{[diagram]} \simeq \text{[diagram]} \xrightarrow{\pi} \text{[diagram]} \xrightarrow{\rho} \text{[diagram]} \\
R_f &= \text{[diagram]} \xrightarrow{\rho^{-1}} \text{[diagram]} \xrightarrow{\pi^{-1}} \text{[diagram]} \\
L_f &= \text{[diagram]} \xrightarrow{\lambda^{-1}} \text{[diagram]} \xrightarrow{\pi^{-1}} \text{[diagram]}
\end{aligned}$$

Note that the 2-morphisms R_m, L_m, R_u, L_u, R_f and L_f can be interpreted as *rotating* their domain, either to the right or the left. For this reason we make the following definition.

Definition 4.8. In $\mathbf{F}(\mathcal{E})$, a 2-morphism is *rotational* if it is composed only from $R_m, L_m, R_u, L_u, R_f, L_f, \sigma_1, \sigma_1^{-1}, \sigma_2, \sigma_2^{-1}$ and interchangers; we write \xrightarrow{R} to denote a composite of rotational generators of length at least 0.

Lemma 4.9. In $\mathbf{F}(\mathcal{E})$, the snake maps satisfy the swallowtail equations:

$$\begin{aligned}
\text{id} &= \text{[diagram]} \xrightarrow{\sigma_1^{-1}} \text{[diagram]} \simeq \text{[diagram]} \xrightarrow{\sigma_2} \text{[diagram]} \\
\text{id} &= \text{[diagram]} \xrightarrow{\sigma_1^{-1}} \text{[diagram]} \simeq \text{[diagram]} \xrightarrow{\sigma_2} \text{[diagram]}
\end{aligned}$$

Proof. Follows easily from the swallowtail equations that form part of the Frobenius presentation \mathcal{F} . See globular.science/1601.002, 5-cells *Pf: Swallowtail 1* and *Pf: Swallowtail 2*. \square

Lemma 4.10. In $\mathbf{F}(\mathcal{E})$, the elements of each pair (R_m, L_m) , (R_u, L_f) , (L_u, R_f) are mutually inverse, up to interchangers and snake maps; that is, the following equations hold:

$$\begin{aligned}
\text{id} &= \text{[diagram]} \xrightarrow{L_m} \text{[diagram]} \xrightarrow{R_m} \text{[diagram]} \simeq \text{[diagram]} \xrightarrow{\sigma_2} \text{[diagram]} \\
\text{id} &= \text{[diagram]} \xrightarrow{R_m} \text{[diagram]} \xrightarrow{L_m} \text{[diagram]} \simeq \text{[diagram]} \xrightarrow{\sigma_1} \text{[diagram]} \\
\text{id} &= \text{[diagram]} \xrightarrow{R_u} \text{[diagram]} \xrightarrow{L_f} \text{[diagram]} \simeq \text{[diagram]} \xrightarrow{\sigma_1} \text{[diagram]} \\
\text{id} &= \text{[diagram]} \xrightarrow{L_u} \text{[diagram]} \xrightarrow{R_f} \text{[diagram]} \simeq \text{[diagram]} \xrightarrow{\sigma_2} \text{[diagram]}
\end{aligned}$$

Proof. See globular.science/1601.002, 5-cells *Pf:* $LmRm=1$, *Pf:* $RmLm=1$, *Pf:* $RuLf=1$ and *Pf:* $LuRf=1$. \square

Lemma 4.11. *In $\mathbf{F}(\mathcal{E})$, the following equations hold:*

$$\begin{aligned} \mu &= \text{diagram} \xrightarrow{L_m, L_f} \text{diagram} \simeq \text{diagram} \xrightarrow{\sigma_1} \text{diagram} \xrightarrow{\lambda} | \\ \nu &= \text{diagram} \xrightarrow{R_m, R_f} \text{diagram} \simeq \text{diagram} \xrightarrow{\sigma_2} \text{diagram} \xrightarrow{\rho} | \end{aligned}$$

Proof. See globular.science/1601.002, 5-cells *Pf:* *Mu Decomposition* and *Pf:* *Nu Decomposition*. \square

Definition 4.12. For a 1-morphism X in $\mathbf{F}(\mathcal{E})$, a chosen (cup, cap) pair are *eliminable* if they match one of the following patterns:

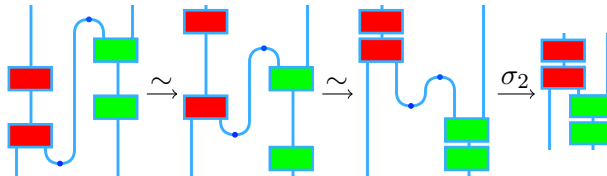


That is, they are directly connected by a central straight wire, and turn in opposite directions. The surrounding diagram may be nontrivial, and the cup and cap may not have adjacent heights.

Definition 4.13. For a 1-morphism X in $\mathbf{F}(\mathcal{E})$, with a chosen eliminable cup and cap pair, the *snake removal scheme* $X \rightarrow X'$ is the following sequence of 2-morphisms:

1. Identify the obstructing generators, which are the components of the diagram lying *between* the cup and cap in height.
2. Gather obstructing generators into maximal groups, with respect to whether they are left or the right of the central wire.
3. Interchange groups vertically beyond the cup or cap.
4. Apply the σ_1 or σ_2 map.

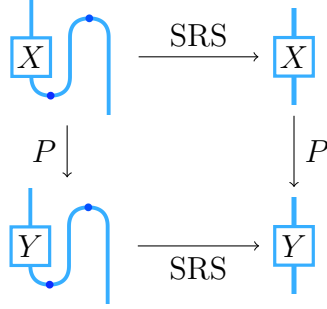
The following graphics explain the scheme. We begin with a central wire with an eliminable cup and cap. First, we identify the obstructing generators, and we gather them into groups as large as possible, which we draw in red to the left of the central wire and in green to the right, giving the first graphic below. Then we interchange red groups up and green groups down, giving in the third graphic. Finally we cancel the cup and cap, giving the final graphic.



Lemma 4.14. *The snake removal scheme is natural with respect to transformations on obstructing groups.*

Proof. In the snake removal scheme, obstructing blocks are acted on by interchangers only, which are natural with respect to transformations of their arguments. \square

Example 4.15. To illustrate this naturalness property, suppose that $P : X \rightarrow Y$ is a 2-morphism in $\mathbf{F}(\mathcal{E})$. Then the following equation holds, where we write SRS for the snake removal scheme:

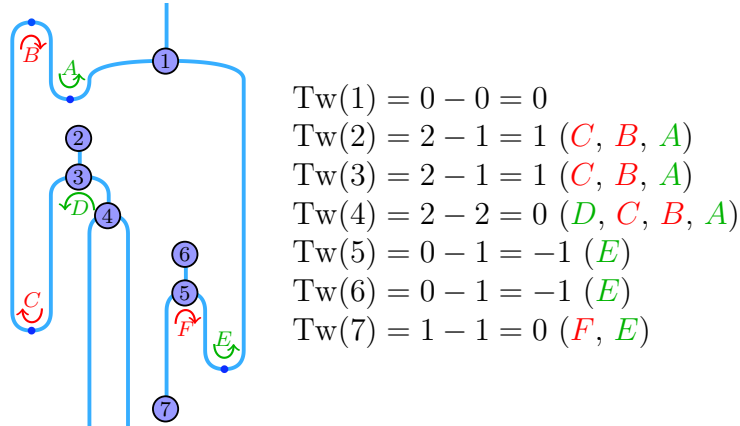


Definition 4.16. A 1-morphism in $\mathbf{F}(\mathcal{E})$ is *connected* or *acyclic*, when its string diagram graph is connected or acyclic, respectively.

Definition 4.17. A *simple* 1-morphism is a 1-morphism in $\mathbf{F}(\mathcal{E})$ which is connected and acyclic, with a unique output wire.

Definition 4.18 (Twistedness). Let X be a simple 1-morphism, and let v be an m , u or f vertex in its string diagram. Then the *twistedness* of v , written $\text{Tw}(v)$, is the number of right turns minus the number of left turns along the shortest path from v to the unique output. We say X is *untwisted* when for all such vertices v , $\text{Tw}(v) = 0$.

Example 4.19. Twistedness is best understood by example. The image below shows a simple 1-morphism with four m vertices (1, 3, 4, 5), one u vertex (7), and two f vertices (2, 6). The arrows show the direction of the shortest path to the output wire at the turning points, with red indicating a right turn, and green a left turn. For each of the numbered vertices, we compute the twistedness as the number of right turns minus the number of left turns.



Note that for computing $\text{Tw}(2)$, D does not count as a left-turn, since we are passing top-to-bottom through vertex 3; but for computing $\text{Tw}(4)$, D does count as we are passing from bottom-right to bottom-left through vertex 3.

Untwisted simple 1-morphisms have some good properties, which we now explore.

Lemma 4.20. *An untwisted simple 1-morphism has no f vertices.*

Proof. Suppose v is an f vertex. Then travelling along the shortest path to the unique output, suppose there are L left turns and R right turns. Since diagram is untwisted $L = R$, and hence $L+R$ is an even number. Also, the only path out of an f vertex begins travelling downwards. So the path begins travelling downwards, turns left or right an even number of times, and finishes at the unique output travelling upwards; a contradiction. \square

Lemma 4.21. *In an untwisted simple 1-morphism, every wire is either straight, or contains an eliminable (cup, cap) pair.*

Proof. Choose a wire W , and let v be the m or u vertex at the end closest to the unique output, and let v' be the m or u vertex at the other end. Write L for the number of left-turns along the path from v' to v , and write R for the number of right turns. Since the composite is untwisted at every vertex, we must have $L = R$. Suppose $L = 0$; then the wire is straight. Suppose $L > 0$; then there must be at least one adjacent “turn left–turn right” or “turn right–turn left” pair along the path from v' to v , and such a pair is eliminable. \square

Definition 4.22. A 1-morphism in $\mathbf{F}(\mathcal{E})$ is in *pseudomonoid form* when it is simple, and formed only from m and u generators, with no f , cup or cap generators.

Lemma 4.23. *A 1-morphism in pseudomonoid form is untwisted.*

Proof. Clearly a 1-morphism in pseudomonoid form is simple. From any m or u vertex, we build a path that travels upwards through the string diagram as far as possible. Suppose we do not reach the unique output at the top of the diagram: then we must have encountered some component with no output legs. But that is impossible, since the 1-morphism is built solely from m and u vertices, which do have output legs. So from any vertex, there is a path to the unique output with no left or right turns; hence the diagram is untwisted. \square

Lemma 4.24. *For every simple 1-morphism X in $\mathbf{F}(\mathcal{E})$, there is a rotational 2-morphism $\Omega_X : X \xrightarrow{R} \tilde{X}$ where \tilde{X} is in pseudomonoid form.*

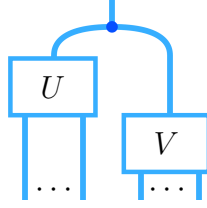
Proof. The generators R_m , R_u and R_f decrease the twistedness of the diagram locally, and L_m , L_u and L_f increase it. We apply these generators repeatedly to obtain a rotational 2-morphism $X \rightarrow X'$, where X' is untwisted. By Lemma 4.20, X' has no f vertices.

The 1-morphism X' is untwisted and simple, so by Lemma 4.21 every wire is either straight, or contains an eliminable cup-cap pair. We now proceed to eliminate every cup and cap, by induction on the total number of cups and caps. Suppose every wire is straight: then we are done. Otherwise, we apply the snake removal scheme of Definition 4.13 to obtain a rotational 2-morphism $X' \rightarrow X''$. Note that X'' contains strictly fewer cups and caps than X' , and is simple since X' is, and is untwisted since it was produced from an untwisted composite by removing an adjacent left-right moving pair. So by induction, we are done, and we have eliminated all cup and cap generators.

The result is in pseudomonoid form, since by construction it is a simple 1-morphism with no f , cup or cap generators. \square

We now define a stronger variant of pseudomonoid form.

Definition 4.25. A 1-morphism in $\mathbf{F}(\mathcal{E})$ is in *left-pseudomonoid form* when it is identical to u , or is identical to the following composite, where U, V are in left-pseudomonoid form:



Lemma 4.26. For any X in pseudomonoid form, $\Theta_X : X \xrightarrow{\sim} \hat{X}$ where \hat{X} is in left-pseudomonoid form.

Proof. We argue by induction on the number of m and u vertices. Suppose $X \equiv u$; then we are done. Otherwise, the uppermost vertex in X is m , and we write L and R for the sets of vertices in the subtrees below the left and right legs of m respectively. We apply interchangers to move all the vertices of L above all the vertices of R . By the inductive hypothesis, we use interchangers to arrange L and R in left-pseudomonoid form, and we are done. \square

Left-pseudomonoid form is useful since it is unaltered by rotational 2-morphisms, as we now explore.

Lemma 4.27. Let X, Y be in left-pseudomonoid form, with $X \xrightarrow{R} Y$. Then $X \equiv Y$.

Proof. Given a simple 1-morphism, its *structure tree* is a binary tree, defined as follows. Start at the unique output, and travel along the path of the string diagram. If you encounter a u or f vertex, append a leaf to the tree. If you encounter an m , append a binary branching, with subtrees given by following the other two legs of the m vertex in a similar way.

By inspection, none of the rotational 2-morphisms change the structure tree of a diagram. Also, it is clear that if two left-pseudomonoid forms have the same structure tree, they are identical. This completes the proof. \square

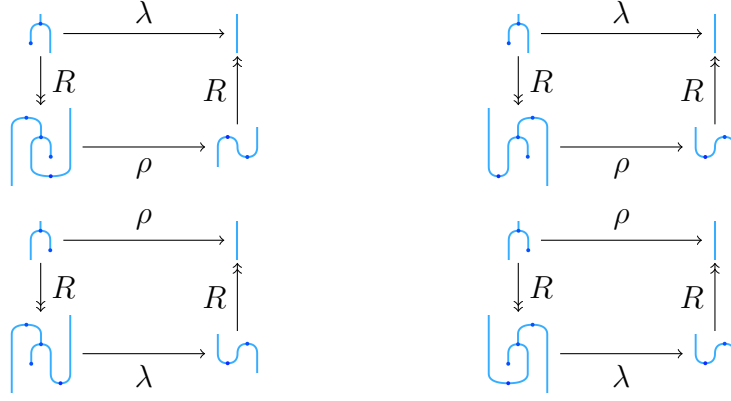
Definition 4.28. In $\mathbf{F}(\mathcal{E})$, the *algebraic* generators are α , λ , ρ and their inverses.

We now give the central proposition, showing how algebraic 2-morphisms can be “untwisted” to act in pseudomonoid form.

Proposition 4.29 (Untwisting). Let $P : X \rightarrow Y$ be a 2-morphism in $\mathbf{F}(\mathcal{E})$ such that X is simple. Then P is equal to a 2-morphism in which the algebraic generators act on untwisted diagrams only.

Proof. We show that the following equations hold in $\mathbf{F}(\mathcal{E})$, where R denotes some composite of rotational generators:





See globular.science/1601.002, *Pf: Left Alpha*, *Pf: Right Alpha*, *Pf: Right Lambda*, *Pf: Left Lambda*, *Pf: Right Rho* and *Pf: Left Rho*. These equations imply a similar set of equations where α^{-1} , λ^{-1} or ρ^{-1} appear at the top of each diagram.

These equations tell us that whenever an algebraic generator acts on a diagram, we can always replace it by a sequence where we twist the diagram locally, apply the algebraic generator, and then twist back. The left-hand equations change the twistedness by -1 , and the right-hand equations change it by $+1$. Note that for α and α^{-1} , depending on the direction of the path to the unique output wire, *two* applications of these equations might be needed to change the twistedness locally by 1 unit. In this way, we can ensure that every algebraic generator γ acts on a part of the diagram that is locally untwisted.

However, our proposition states that the *entire* diagram on which γ acts should be untwisted. Suppose $\gamma : X \rightarrow Y$ is a single algebraic 2-morphism within the composite P , acting on a locally untwisted part of the diagram. Then by Lemma 4.14, the following equation holds:

$$\begin{array}{ccc} X & \xrightarrow{\gamma} & Y \\ \Omega_X \downarrow & & \uparrow \Omega_Y^{-1} \\ \tilde{X} & \xrightarrow{\gamma} & \tilde{Y} \end{array} \quad (6)$$

We use this to replace every algebraic generator acting on a locally untwisted part of the diagram, with the same algebraic generator acting on a completely untwisted diagram. \square

4.3 Coherence

We now give the coherence theorems.

Proposition 4.30 (Coherence for snakeorators). *In $\mathbf{F}(\mathcal{E})$, let $P, Q : X \rightarrow Y$ be composites of snakeorators, inverse snakeorators and interchangers, such that X is a connected 1-morphism. Then $P = Q$.*

Proof. Since composites of this type are invertible, we may assume $X = Y$ and $Q \equiv \text{id}$. The composite P is formed from σ_1 , σ_2 , σ_1^{-1} , σ_2^{-1} and interchanger maps. The source of the σ_1^{-1} and σ_2^{-1} maps is the identity, so by naturality, they can all be moved to the beginning of the composite. Similarly, the σ_1 and σ_2 maps can all be moved to the end of the composite. So our rearranged composite is of the following

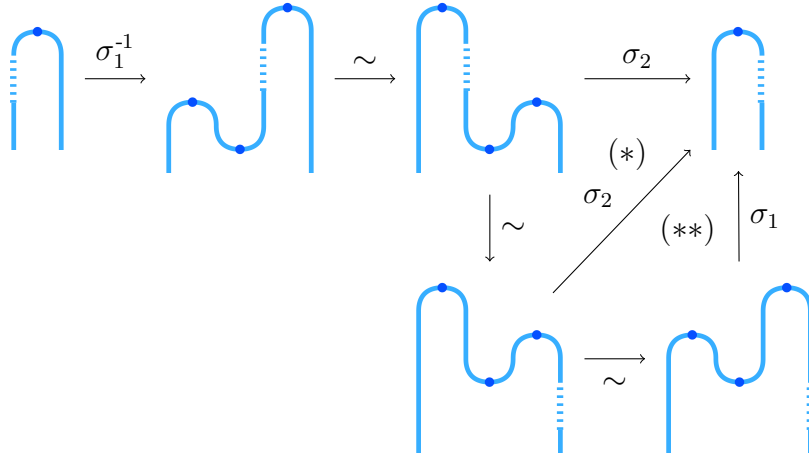


Figure 7: Turning σ_2 into σ_1 in a general composite

form: a sequence of inverse snakeorators, followed by a sequence of interchangers, followed by a sequence of snakeorators.

We argue by induction on the number of inverse snakeorator generators. This proof will have two inductive arguments: we call this first one I_1 . Suppose there are no inverse snakeorators: then we are done. Otherwise, write F for the final inverse snakeorator present in the rearranged composite. Suppose for the rest of the proof that it is a σ_1^{-1} generator; for a σ_2^{-1} generator, a similar proof applies.

The final inverse snakeorator F produces a single cup and cap, at least one of which will be annihilated later in the composite, since the target of P has as many cups and caps as the source of P . There are two ways that this can happen: either (A) they are annihilated with each other by a σ_1 generator, or (B) one of them is annihilated with a neighbouring cup or cap by a σ_2 generator. Suppose case (B) holds; then we will show our composite is equal to one in which (A) in fact holds. The argument is illustrated in Figure 7. We begin with some composite that contains a cap. At some point lower down the left-hand wire, a σ_1^{-1} generator acts to create a new cup and cap pair. Later in the composite, following the application of interchangers, and snakeorators to other cups and caps not displayed, a σ_2 generator is applied to the right-hand cup and cap. (We are supposing that it is the newly-created *cup* which is annihilated first; if the newly-created cap is annihilated first, a reflected argument applies.) In triangle (*), we observe by naturality that the composite is equal to one in which the σ_2 is applied higher up, adjacent to the leftmost cap. In triangle (**), we apply one of the swallowtail equations to replace the σ_2^{-1} with a σ_1^{-1} that annihilates the same cup and cap created in the first arrow of the diagram.

We assume therefore that case (A) holds. Local to the cup and cap produced by F , the diagram will look like this:

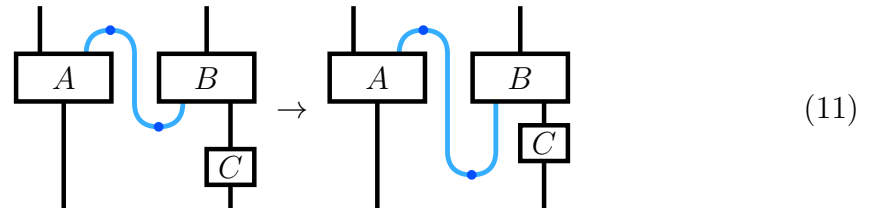
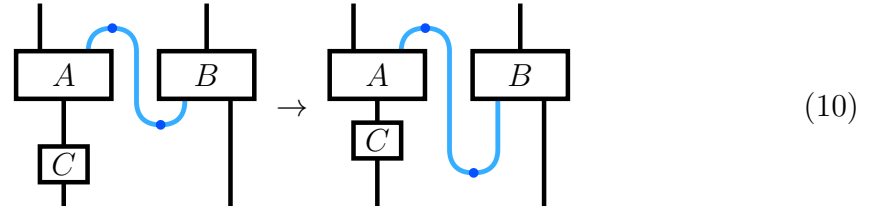
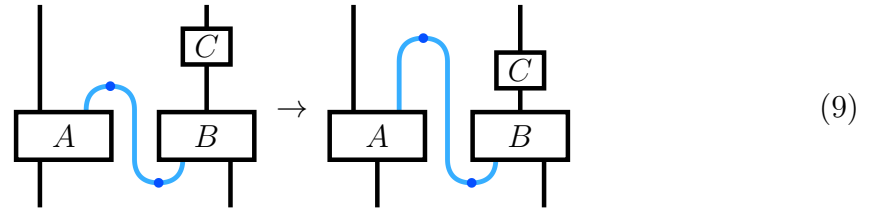
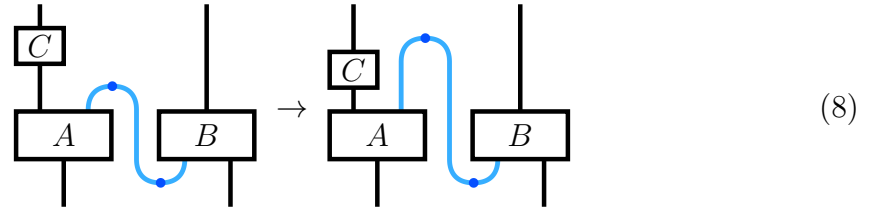
$$\left| \begin{array}{c} \sigma_1^{-1} \\ \rightarrow \end{array} \right. \text{cup and cap} \xrightarrow{\sim, \sigma_1, \sigma_2} \text{cup and cap} \xrightarrow{\sigma_1} \left| \right. \quad (7)$$

The central arrow represents some composite of interchangers, σ_1 and σ_2 generators. By assumption, the σ_1 and σ_2 maps will act only on the rest of the diagram, not

the displayed cups and caps, but the interchangers may affect any part of the diagram. Since this central arrow is not the identity, we cannot immediately apply the invertibility equation to cancel the σ_1^{-1}, σ_1 pair from the composite.

During the course of this central arrow, the chosen cup and cap may become separated vertically, with the cap always remaining above the cup.¹ Since the initial and final separation is clearly 0, this separation must have some maximum value $n \in \mathbb{N}$ over the course of the central arrow. We now show that our composite is equal to one for which this maximum value is 0. We give an inductive argument I_2 , jointly on the value n of this maximum, and its multiplicity m over the course of the central arrow (since the separation may reach its maximum value of n more than once over the composite.)

There are 4 ways that the separation between the cup and cap can increase, by applying interchangers as follows, where the boxes A and B indicate arbitrary composites, the box C is a composite of height 1 (i.e. a generator padded on the left and right), and the black wires are arbitrary types:



In each case the separation increases by 1 unit. After this increase, arbitrary interchangers can take place in the diagram, not involving the cup and cap; this will leave the separation invariant. Finally, the separation will decrease, giving the end of the local maximum. It could decrease by the reverse of one of the processes (8–11) (4 ways); or by a snakeorator being applied in a region between the cup and cap in height, on the left or the right of the central blue wire (2 ways).

¹The cap could only go below the cup if an additional inverse snakeorator σ_2^{-1} was applied to the central connecting wire, but by assumption σ is the final inverse snakeorator present in the composite.

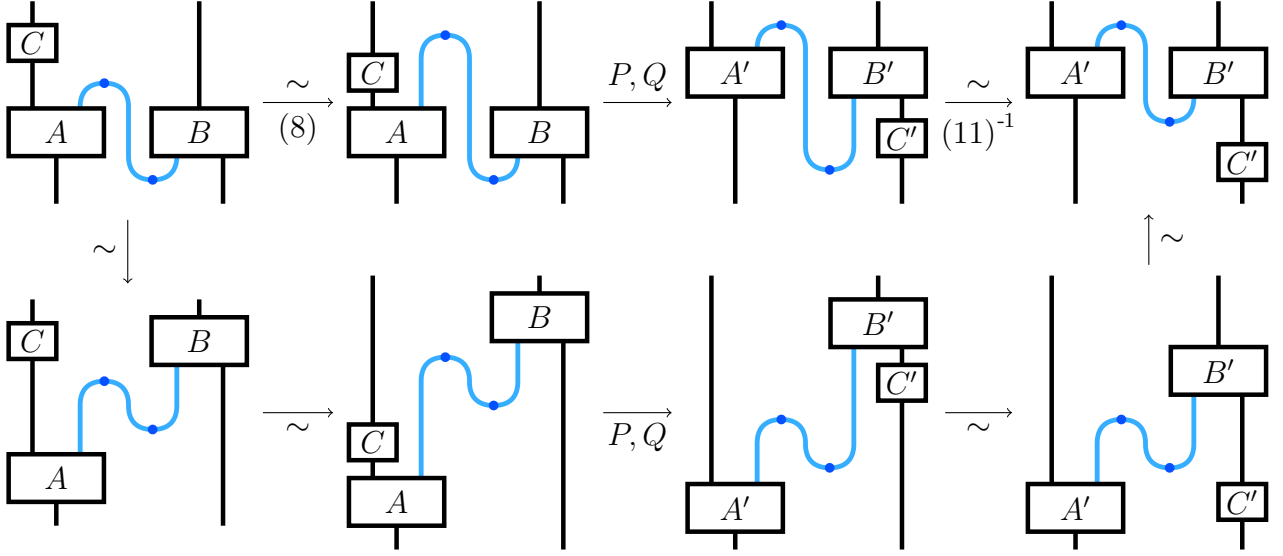


Figure 8: Reducing the local maximum separation between a cup and cap

So in total there are 4 ways for the separation to increase, and 6 ways for it to decrease, giving a total of 24 types of local maximum. For each case, suppose the separation increases from n to $n + 1$, and then decreases from $n + 1$ to at most n . Then we can show directly that this is equal to a composite in which the separation is at most n throughout. While the number of cases is large, they are all handled straightforwardly and in a similar way.

We analyze one case in detail. Suppose that the separation increases from n to $n + 1$ by method (8); followed by 2-morphisms P, Q applied between the cup and cap in height, to the left and right of the central wire respectively; followed by the separation decreasing from $n + 1$ to at most n by method (11). (2-morphisms applied above the cap or below the cup may be moved later in the composite by naturality, and we neglect them.) Then by the argument in Figure 8, we can perform the operations in a different order, under which the separation is at most n . Commutativity of this diagram, and others like it for the different cases, follows from naturality of the interchanger in a monoidal bicategory.

By this argument, we have reduced the multiplicity of local maxima of the separation by 1; or, if the multiplicity was already 1, we have reduced the global maximum. By the hypothesis of the inductive argument I_2 , we are done.

We have demonstrated that the composite in (7) is equal to one in which we apply σ_1^{-1} , act only on the cups and caps by interchanging them as a single unit, and then apply σ_1 . By naturality of the interchanger, the σ_1 and σ_1^{-1} can now be cancelled. Thus we have shown that our composite is equal to one with strictly fewer inverse snakeoperators. By the hypothesis of the inductive argument I_1 , we are done. \square

Proposition 4.31 (Coherence for rotational 2-morphisms). *In $\mathbf{F}(\mathcal{E})$, let $P, Q : X \xrightarrow{R} Y$ be rotational 2-morphisms, such that X is simple. Then $P = Q$.*

Proof. Note that the rotational 2-morphisms are invertible, so $P = Q$ just when $Q^{-1} \circ P = \text{id}_X$; so it is enough to consider the case that $Y = X$ and $Q = \text{id}_X$. Also, by Lemma 4.24, there is a rotational isomorphism $\Omega_X : X \rightarrow \tilde{X}$, where \tilde{X} is

in pseudomonoid form; so without loss of generality, we may suppose that X is in pseudomonoid form, and therefore untwisted by Lemma 4.23.

Let v be any m vertex in X . Since R_m and L_m maps act locally on multiplication vertices, and no rotational cells can introduce or eliminate m vertices, we can move all R_m and L_m instances acting on v to the beginning of the composite P . Since the source and target of P is untwisted, an equal number of R_m and L_m 2-morphisms must act on it, since they change the twistedness locally; we cancel adjacent (R_m, L_m) and (L_m, R_m) pairs using Lemma 4.10, at the cost of introducing additional snakeors. Similarly, each u vertex in X will be rotated by a succession of R_u , L_u , R_f and L_f maps; as for the m vertices, we move these to the beginning of the composite, and eliminate them pairwise. Hence we obtain $P = P' : X \Rightarrow X$, where P' is formed purely of interchangers and snake maps. But then by Proposition 4.30, we conclude $P' = \text{id}$. \square

Lemma 4.32. *In $\mathbf{F}(\mathcal{E})$, suppose X, Y are 1-morphisms in pseudomonoid form, and $X \xrightarrow{R} Y$. Then $X \xrightarrow{\sim} Y$.*

Proof. Consider the following diagram:

$$\begin{array}{ccc} X & \xrightarrow{R} & Y \\ \Theta_X \searrow & & \nearrow \Theta_Y^{-1} \\ & \hat{X} = \hat{Y} & \end{array} \quad (12)$$

The 2-morphisms Θ_X and Θ_Y are defined by Lemma 4.26, and are composed purely of interchangers. The equality at the bottom follows from Lemma 4.27. By Proposition 4.31, the diagram commutes. Since the lower path $X \xrightarrow{\sim} \hat{X} = \hat{Y} \xrightarrow{\sim} Y$ is composed purely of interchangers, the result follows. \square

Theorem 4.6. (Coherence for Frobenius structures.) *Let $P, Q : X \rightarrow Y$ be 2-morphisms in $\mathbf{F}(\mathcal{F})$, such that X is connected and acyclic, with at least one input or output. Then $P = Q$.*

Proof. Let X be a simple 1-morphism in $\mathbf{F}(\mathcal{F})$, and let $P, Q : X \rightarrow Y$ be 2-morphisms. Since the 2-morphisms of $\mathbf{F}(\mathcal{F})$ are invertible, then $P = Q$ just when $Q^{-1} \circ P = \text{id}$; so it is enough to consider the case that $X = Y$ and $Q = \text{id}$. We then proceed as follows.

- Define $P_1 : X \rightarrow X$ as the image of P under the embedding $\mathbf{F}(\mathcal{F}) \rightarrow \mathbf{F}(\mathcal{E})$. It is enough for us to prove $P_1 = \text{id}$, since \mathcal{F} and \mathcal{E} are equivalent presentations.
- Define P_2 by taking P_1 and eliminating all instances of μ and ν using Lemma 4.11.
- Define P_3 by taking P_2 and ensuring all algebraic generators act on untwisted diagrams only, using Proposition 4.29.
- Define $P_4 := \Omega_X \circ P_3 \circ \Omega_X^{-1} : \tilde{X} \rightarrow \tilde{X}$.

Clearly $P_1 = P_2 = P_3$, and $P_3 = \text{id}$ just when $P_4 = \text{id}$.

We now consider the structure of P_4 . Its source and target are in pseudomonoid form, and P_4 itself is built from rotational 2-morphisms, along with algebraic

2-morphisms acting on diagrams of pseudomonoid form. That is, P_4 is of the following form, where X_i and Y_i are of pseudomonoid form, γ_i are algebraic 2-morphisms, and R indicates a composite rotational 2-morphism:

$$P_4 = X_0 \xrightarrow{R} Y_0 \xrightarrow{\gamma_0} X_1 \xrightarrow{R} Y_1 \xrightarrow{\gamma_1} \dots \xrightarrow{R} Y_n = X_0$$

By applying Lemma 4.32, we can build P_5 as follows, with $P_4 = P_5$:

$$P_5 = X_0 \xrightarrow{\sim} Y_0 \xrightarrow{\gamma_0} X_1 \xrightarrow{\sim} Y_1 \xrightarrow{\gamma_1} \dots \xrightarrow{\sim} Y_n = X_0$$

This composite lies purely in the image of the pseudomonoid presentation \mathcal{P} . But then by the coherence theorem for pseudomonoids, we conclude $P_5 = \text{id}$; see the work of Lack [19], and the thesis of Houston [12, Section 6].

In the statement of the theorem, we required only that X had a single input and output. To reduce to the case of a unique output, one can compose with cups and caps appropriately; the swallowtail equations ensure this gives a bijection of hom-sets. \square

4.4 Adjoints

We now consider the case that the generators m, u have adjoints.

Definition 4.33. The *right-adjoint Frobenius presentation* \mathcal{F}^* is defined to be the Frobenius presentation \mathcal{F} , with the following additional data:

- Additional 1-morphisms m^* and u^* :

$$\begin{array}{c} \text{---} \cup \text{---} \\ \text{---} \end{array} \quad \begin{array}{c} \bullet \\ \text{---} \end{array} \quad (13)$$

- Additional 2-morphisms $\eta, \epsilon, \phi, \psi$:

$$\begin{array}{c} \text{---} \text{---} \xrightarrow{\eta} \begin{array}{c} \text{---} \cup \text{---} \\ \text{---} \end{array} \\ \text{---} \end{array} \quad \begin{array}{c} \begin{array}{c} \cup \\ \text{---} \end{array} \xrightarrow{\epsilon} \text{---} \end{array} \quad (14)$$

$$\begin{array}{c} \text{---} \xrightarrow{\phi} \bullet \\ \text{---} \end{array} \quad \begin{array}{c} \begin{array}{c} \bullet \\ \text{---} \end{array} \xrightarrow{\psi} \text{---} \end{array} \quad (15)$$

- Additional equations, stating that $m \dashv m^*$ and $u \dashv u^*$:

$$\text{id} = \begin{array}{c} \text{---} \cup \text{---} \\ \text{---} \end{array} \xrightarrow{\eta} \begin{array}{c} \cup \\ \text{---} \end{array} \xrightarrow{\epsilon} \text{---} \quad \text{id} = \begin{array}{c} \text{---} \xrightarrow{\eta} \bullet \xrightarrow{\epsilon} \text{---} \end{array} \quad (16)$$

$$\text{id} = \begin{array}{c} \text{---} \cup \text{---} \\ \text{---} \end{array} \xrightarrow{\eta} \begin{array}{c} \cup \\ \text{---} \end{array} \xrightarrow{\epsilon} \text{---} \quad \text{id} = \begin{array}{c} \text{---} \xrightarrow{\eta} \bullet \xrightarrow{\epsilon} \text{---} \end{array} \quad (17)$$

Definition 4.34. In $\mathbf{F}(\mathcal{F}^*)$, define the following composites:

$$\begin{array}{c} \text{---} \cup \text{---} \\ \text{---} \end{array} := \begin{array}{c} \text{---} \cup \text{---} \\ \text{---} \end{array} \quad \begin{array}{c} \bullet \\ \text{---} \end{array} := \begin{array}{c} \cup \\ \text{---} \end{array} \quad (18)$$

Lemma 4.35. *In $\mathbf{F}(\mathcal{F}^*)$, we have the following adjunctions:*



Proof. The first row of adjunctions are explicit in the definition of \mathcal{F}^* . The second row are constructed straightforwardly from the available data. \square

4.5 Graphical calculus for Frobenius pseudomonoids

As a result of the coherence theorem, we can relax our conventions for the graphical calculus for a Frobenius pseudomonoid. For any number of input and output wires (as long as there is at least one in total), we may draw a generic vertex that connects them:



By the coherence theorem, we are guaranteed that all acyclic, connected ways of forming a composite with this type will be canonically isomorphic, so we may as well draw this simpler vertex to represent the entire isomorphism class. Furthermore, given any two connected acyclic 1-morphisms with boundary in $\mathbf{F}(\mathcal{F})$, there is a canonical choice of morphism between them, which in the surface calculus we can show as a pointlike operation, such as expression (1).

For the right-adjoint Frobenius presentation \mathcal{F}^* , we have additional graphical components available thanks to the adjunctions described in Lemma 4.35.

4.6 *-Autonomous categories

From the work of Street [27], it is known that the following definition of non-symmetric $*$ -autonomous category agrees with that of Barr [2], up to a Cauchy-completeness assumption. Here **Prof** is the symmetric monoidal bicategory of categories, profunctors and natural transformations [6].

Definition 4.36. A $*$ -autonomous category is a pseudomonoid $(\mathbf{C}, m, u, \alpha, \lambda, \rho)$ in **Prof**, equipped with a morphism $f : \mathbf{C} \rightarrow \mathbf{1}$ such that $f \circ m : \mathbf{C} \times \mathbf{C} \rightarrow \mathbf{1}$ is a biexact pairing, and such that m and u have right adjoints.

Proposition 4.37. *The data of a $*$ -autonomous category is equivalent to that of an \mathcal{F}^* -structure in **Prof**.*

Proof. The reverse direction immediate, since given an \mathcal{F}^* -structure in **Prof**, the composite $f \circ m$ is clearly biexact, thanks to the invertible 2-morphisms μ and ν .

For the forward direction, we sketch the main idea. In Definition 4.36, the biexact pairing condition means that if one composes the right leg of $f \circ m : \mathbf{C} \times \mathbf{C} \rightarrow \mathbf{1}$ with the Hom-profunctor of type $\mathbf{1} \rightarrow \mathbf{C} \times \mathbf{C}^{\text{op}}$, the resulting profunctor of type $\mathbf{C} \rightarrow \mathbf{C}^{\text{op}}$ is an equivalence. Therefore, this definition is in terms of *two* objects, \mathbf{C} and \mathbf{C}^{op} , and structures defined on them. But since \mathbf{C} and \mathbf{C}^{op} are equivalent, it stands to reason that we can transport any structures defined on \mathbf{C}^{op} across to \mathbf{C} , yielding a definition in terms of \mathbf{C} alone. This is an algorithmic procedure, and the result is an \mathcal{F}^* -algebra in **Prof**. \square

We now prove our main theorem.

Theorem 2.2. *Two sequent proofs in multiplicative linear logic have equal interpretations in the free $*$ -autonomous category just when their surfaces diagrams are equivalent.*

Proof. The generators in Figure 1, and the equations in Figure 2, are precisely the definition of an \mathcal{F}^* -structure rendered in the surface calculus. (In fact they are redundant, since they include additional adjunction equations which Lemma 4.35 shows are already derivable.) Under the equivalence of Proposition 4.37, it is essentially immediate that this reduces to the standard interpretation of the sequent calculus in a $*$ -autonomous category [25]: CUT is by composition and AXIOM is the identity morphism, mediated by the adjunctions $V_* \dashv V^*$ of profunctors induced by a variable defined by a functor $V : \mathbf{1} \rightarrow \mathbf{C}$; (\otimes, I) is the monoidal product of the $*$ -autonomous category; the negations come from the biclosed structure; and (\wp, \perp) is the dual monoidal structure induced by negation. \square

References

- [1] K. Bar, A. Kissinger, and J. Vicary. The *Globular* proof assistant. ncatlab.org/nlab/show/Globular.
- [2] M. Barr. Nonsymmetric $*$ -autonomous categories. *Theoretical Computer Science*, 139(1-2):115–130, mar 1995.
- [3] J. W. Barrett, C. Meusburger, and G. Schaumann. Gray categories with duals and their diagrams. *J. Diff. Geom., to appear*. arXiv:1211.0529.
- [4] B. Bartlett. Quasistrict symmetric monoidal 2-categories via wire diagrams. 2014. arXiv:1409.2148.
- [5] R. Blute, J. Cockett, R. Seely, and T. Trimble. Natural deduction and coherence for weakly distributive categories. *JPAA*, 113(3):229–296, 1996.
- [6] F. Borceux. *Handbook of Categorical Algebra: Volume 1, Basic Category Theory*. Cambridge University Press, 1994.
- [7] R. Di Cosmo and D. Miller. Linear logic. In E. N. Zalta, editor, *The Stanford Encyclopedia of Philosophy*. Summer 2015 edition, 2015.
- [8] C. Douglas and A. Henriques. Internal bicategories. arXiv:1206.4284, 2012.
- [9] J.-Y. Girard. Linear logic. *TCS*, 50(1):1–101, 1987.
- [10] A. Guglielmi. *All about Proofs, Proofs for All*, chapter Deep Inference, pages 164–172. College Publications, 2015. Online.
- [11] W. Heijltjes and R. Houston. No proof nets for MLL with units. In *Proceedings of CSL-LICS 2014*.
- [12] R. Houston. *Linear logic without units*. PhD thesis, University of Manchester, 2007. arXiv:1305.2231.

- [13] D. Hughes. Deep inference proof theory equals categorical proof theory minus coherence. Unpublished note. Online, 2004.
- [14] D. Hughes. Simple multiplicative proof nets with units. arXiv:math/0507003, 2005.
- [15] D. Hughes. Simple free star-autonomous categories and full coherence. *JPAA*, 216(11):2386–2410, 2012.
- [16] B. Hummon. *Surface diagrams for Gray categories*. PhD thesis, UC San Diego, 2012. Online.
- [17] A. Joyal and R. Street. The geometry of tensor calculus, I. *Adv. Math.*, 88(1):55–112, 1991.
- [18] G. M. Kelly and S. MacLane. Coherence in closed categories. In *Saunders Mac Lane Selected Papers*, pages 471–514. 1979.
- [19] S. Lack. A coherent approach to pseudomonads. *Adv. Math.*, 152(2):179–202, 2000.
- [20] S. Lack. Composing PROPs. *TAC*, 13(9):147–163, 2004. Online.
- [21] P.-A. Melliès. A topological correctness criterion for multiplicative non-commutative logic. In *Linear Logic in Computer Science*, pages 283–322. Cambridge University Press (CUP).
- [22] P.-A. Melliès. *Interactive models of computation and program behaviour*, chapter Categorical Semantics of Linear Logic. 2009.
- [23] P. Pstragowski. On dualizable objects in monoidal bicategories. Master’s thesis, Bonn University, 2014. arXiv:1411.6691.
- [24] C. Schommer-Pries. *The Classification of Two-Dimensional Extended Topological Field Theories*. PhD thesis, Department of Mathematics, University of California, Berkeley, 2009. arXiv:1112.1000.
- [25] R. A. G. Seely. *Categories in Computer Science and Logic*, chapter Linear logic, *-autonomous categories and cofree coalgebras, pages 371–382. AMS, 1989.
- [26] S. Slavnov. From proof-nets to bordisms: the geometric meaning of multiplicative connectives. *MSCS*, 15(06):1151, 2005.
- [27] R. Street. Frobenius monads and pseudomonoids. *J. Math. Phys.*, 45(10):3930, 2004.